J Membrane Biol (2010) 237:107–114
DOI 10.1007/s00232-010-9311-0

First-Leaflet Phase Effect on Properties of Phospholipid Bilayer Formed Through Vesicle Adsorption on LB Monolayer

Jin-Won Park

Received: 11 July 2010 / Accepted: 20 October 2010 / Published online: 1 November 2010
© Springer Science+Business Media, LLC 2010

Abstract Phospholipid bilayers were formed on mica using the Langmuir–Blodgett technique and liposome fusion, as a model system for biomembranes. Nanometer-scale surface physical properties of the bilayers were quantitatively characterized upon the different phases of the first leaflets. Lower hydration/steric forces on the bilayers were observed at the liquid phase of the first leaflet than at the solid phase. The forces appear to be related to the low mechanical stability of the lipid bilayer, which was affected by the first leaflet phase. The first leaflet phase also influenced the long-range repulsive forces over the second leaflet. Surface forces, measured using a modified probe with an atomic force microscope, showed that lower long-range repulsive forces were also found at the liquid phase of the first leaflet. Force measurements were performed at 300 mM sodium chloride solution so that the effect of the phase on the long-range repulsive forces could be investigated by reducing the effect of the repulsion between the second-leaflet lipid headgroups on the long-range repulsive forces. Forces were analyzed using the Derjaguin–Landau–Verwey–Overbeek theory so that the surface potential and surface charge density of the lipid bilayers were quantitatively acquired for each phase of the first leaflet.

Keywords Langmuir–Blodgett film · Membrane biophysics · Membrane electrostatics · Planar bilayer

J.-W. Park (✉)
Department of Chemical Engineering, School of Engineering, Seoul National University of Science and Technology, 172 Gongreung2dong, Nowonku, Seoul 173-743, South Korea
e-mail: jwpark@snut.ac.kr

Introduction

Many efforts have been devoted to the study of the physicochemical properties of the lipid layer in recent years since they are important to understanding specific membrane functions including molecular recognition, cell adhesion, cell fusion and intercellular communication (McConnell et al. 1986; Sackmann 1996; Boxer 2000; Garcia-Manyes et al. 2005). Supported lipid layers on solid substrates are known as well-defined models of the cell surface and can be used to investigate molecular events in membranes because very sensitive analytical techniques can be applied (McConnell et al. 1986; Sackmann 1996; Boxer 2000). Supported lipid layers have been used in many areas of biomedical research such as cell recognition, membrane-mediated catalysis, effects of anesthetics and antimicrobial peptides (Brian and McConnell 1984; Giesen et al. 1991; Mou et al. 1994; Miszta et al. 2008).

Atomic force microscopy (AFM) has proven to be a strong method for measuring the forces of interaction between the AFM probe and the surface, giving information on the physical properties of a sample surface (Biggs 1995; Fang et al. 2000; Beech et al. 2002; Engler et al. 2004). As the AFM probe tip approaches the sample, repulsive forces can be measured, such as electrostatics, salvation, hydration and compression-related steric forces. The retraction force curves often show a hysteresis, referred to as an "adhesion pull-off event," which can be used to estimate the adhesion forces. Much experimental force data are now available in the literature, and theoretical models have been introduced for the analysis of forces acting between two solid surfaces (Senden et al. 1994; Van der Vegte and Hadziioannou 1997; Cappella and Dietler 1999; Dimitriadis et al. 2002; Franz et al. 2002; Butt and Franz 2002; Loi et al. 2002).

In biological systems, cell membranes have an asymmetrical distribution across the bilayer of the membranes. Phosphatidylethanolamine (PE) is the predominant lipid species in the inner leaflet, while the outer leaflet has more phosphatidylcholine (PC) (Boon and Smith 2002a, b). This asymmetry is a key feature of cell plasma membranes for exocytosis, intracellular fusion, lipid–protein interactions and signal transduction, which are also associated with structural heterogeneity (Brown and London 2000; Bagatolli and Gratton 2000; Rinia et al. 2001; De Almeida et al. 2002; Tokumasu et al. 2003; Devaux and Morris 2004). Still, little is known about how the first-leaflet phase can affect quantitatively the physical properties of the lipid bilayer, i.e., hydration/steric repulsion, adhesion and electrostatic properties. In this work, we investigated the properties of the lipid layer.

Experiments

Dipalmitoylphosphatidylethanolamine (DPPE), dioleoylphosphatidylethanolamine (DOPE), dipalmitoylphosphatidylcholine (DPPC), dioleoylphosphatidylcholine (DOPC), dipalmitoylphosphatidylglycerol (DPPG) and dioleoylphosphatidylglycerol (DOPG) were purchased from Avanti Polar Lipids (Alabaster, AL) and used without further purification. Langmuir–Blodgett (LB) films were prepared at 25°C with a KSV 5000 LB system (KSV Instruments, Helsinki, Finland). Lipids were dissolved at 0.5 mM in chloroform/methanol (4:1). Monolayers were spread on 300 mM sodium chloride subphase at pH 4, and after evaporation of the solvent, they were compressed at a rate of 10 mm/min. All layers were deposited at a constant surface pressure of 25 mN/m by raising mica through the air–water interface, after the mica was attached to a 15-mm-diameter magnetic plate and cleaned. Transfer ratios were 1:1. All layers were used to confirm the phase difference, but the layers of DPPE and DOPE were used as a first leaflet where the second leaflets of DPPC–DPPG and DOPC–DOPG were, respectively, formed through liposome fusion after the mica was transferred on the AFM stage. More description is presented in "Results and Discussion" section.

Large unilamellar vesicles (LUVs) were prepared with 1.5:1 of DPPC–DPPG and 1.5:1 of DOPC–DOPG, respectively (Park 2007). Lipids were well mixed in chloroform/methanol (4:1) to a total lipid concentration of 10 mg/ml. The glass surface of a vial was coated with these lipids by evaporation of the solvent under a stream of nitrogen during vortexing. Traces of solvent were removed under vacuum for 3–4 h. Lipids were resuspended in 300 mM sodium chloride at pH 4. During resuspension, the lipid concentration was adjusted to 2 mg/ml. This solution was subjected to 10 freeze–thaw cycles, with thaw performed above the transition temperature of each lipid. After the freeze–thaw cycles, the lipids form multilamellar vesicles (MLVs). MLVs were transferred into an extruder (Avanti Polar Lipids) and extruded through a standard polycarbonate filter (Osmonic, West Borough, MA). Vesicles were extruded 10 times through a 0.1-μm pore size double polycarbonate filter above the transition temperature.

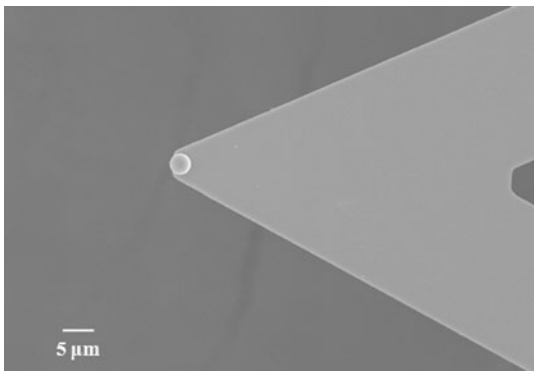

Fig. 1 Silica sphere-attached cantilever

AFM measurements were made at 25°C using an optical lever microscope equipped with a liquid cell (3D MFP; Asylum Research, Santa Barbara, CA) and a temperature controller. Contact-mode topographic images were taken in the constant-deflection mode using oxide-sharpened, microfabricated Si_3N_4 cantilevers (Olympus, Tokyo, Japan) with a typical radius of curvature of 20 nm and spring constants of 0.03 and 0.5 N/m (manufacturer specified). The mica was placed onto a Petri dish put on a magnetic place so that it was held tightly to the AFM stage by magnetic force. The AFM cantilever was mounted onto the cell and carefully lowered to the lipid bilayers, after the vesicle solution was injected into the dish with a waiting period of 1 h for liposome fusion to form lipid bilayer on the mica above the transition temperature. At contact-mode AFM, surface force measurements were made with the cantilever at 1 Hz. The sensitivity of the AFM detector was estimated using the slope of the loading curve. For quantitative electrostatic-property analysis, a silica sphere-attached cantilever, shown in Fig. 1, was used for other surface force measurements.

Theory

Theories describing the forces between interacting electrostatic double layers have been considered by numerous authors. The interaction between similarly charged double layers at low surface potentials is described by the theory of Derjaguin–Landau–Verwey–Overbeek (DLVO) (Derjaguin 1940). According to the DLVO theory, the total interaction energy between two plates can be considered as

the sum of several contributions, including an attractive van der Waals component (V_A) and an electrostatic repulsion or attraction (V_E). There is also considerable evidence for an additional repulsion (V_S) at close separations resulting from the presence of ordered solvent layers (Israelachvili and Adams 1978; Shuin and Kekicheff 1993; Parker and Christenson 1988; O'Shea et al. 1994).

Using the Derjaguin (1934) approximation, the force between spheres of radius R_T can be related to the energy between plates by the expression

$$F/R_T = 2\pi(V_A + V_E + V_S). \quad (1)$$

The van der Waals energy (V_A) in the nonretarded limit is described by an equation of the form

$$V_A = -A_H/12\pi d^2, \quad (2)$$

where A_H is the Hamaker constant and d is the separation distance (Hartmann 1991). The Hamaker constant of the lipids is assumed to be 7.0×10^{-20} J since the largest component of the layer is hydrocarbon (Israelachvili 1991). The Hamaker constant used for the SiO_2 surface is 0.8×10^{-20} J (Ducker et al. 1992). The electrostatic interaction (V_E) can be derived by considering the free energy associated with the formation of a double layer or by integrating the electrostatic force (Verwey and Overbeek 1948; Hogg et al. 1966; Hunter 1987). Using the latter method, the interaction for a 1:1 electrolyte is

$$V_E = -\int_{\infty}^{D} \left\{ 2n^0 kT \left[\cosh\left(\frac{ze\psi}{kT}\right) - 1 \right] - \frac{\varepsilon}{2}\left(\frac{d\psi}{dz}\right)^2 \right\} dz, \quad (3)$$

where ψ is the electrostatic potential. The first term in Eq. 3 is a repulsive osmotic component that results from the accumulation of charge in the gap between the plates, and the second is a Maxwellian stress that represents an induced charge and is always attractive. For similarly charged surfaces, the second term disappears, leaving a result equivalent to the DLVO theory. To determine V_E explicitly, the electrostatic potential must be known. This can be found by solving the Poisson–Boltzmann equation:

$$\frac{d^2\psi}{dz^2} = -\frac{1}{\varepsilon_0 \varepsilon_r} \sum_i n_i^0 z_i e \exp\left(-\frac{z_i e\psi}{kT}\right). \quad (4)$$

Generally, the complete nonlinear form of Eq. 4 must be solved, which can be accomplished only by numerical techniques (Chan et al. 1980). Integration of Eq. 3 was then achieved with Simpson's 3/8 rule. The additional repulsive force (V_S) in Eq. 1 is thought to arise from the presence of ordered solvent layers and can be described by a decaying oscillatory force (Parker 1994). The nature of this repulsive force is not clearly understood and will be neglected in the calculations presented here.

Results and Discussion

Toward the goal of investigating the first leaflet phase effect on the physical properties of the bilayers, the second phospholipid layer on the first phospholipid layer made earlier with the LB technique was formed through liposome fusion. Four types of lipid bilayers could be made: DPPC–DPPG/DPPE, DPPC–DPPG/DOPE, DOPC–DOPG/DPPE and DOPC–DOPG/DOPE (A-B/C; A-B is assigned to the second leaflet, and C is assigned to the first leaflet). The schematic drawings of these lipid bilayers are presented in Fig. 2. The phase difference of DPPE and DOPE was first confirmed using the surface pressure (π) versus area isotherms (25°C) of DPPE, DOPE and DPPE–DOPE monolayers at the air–water interface (Fig. 3). The shapes of the isotherms indicate that the saturated DPPE monolayer is characterized by a two-dimensional (2D) solid-like organization, whereas the unsaturated DOPE monolayer has a 2D liquid-like behavior. The isotherm for the mixed DPPE–DOPE monolayer falls in the middle of those for the pure lipid monolayers.

Force measurements were performed with the cantilever at 25°C on the lipid bilayer in 300 mM sodium chloride at

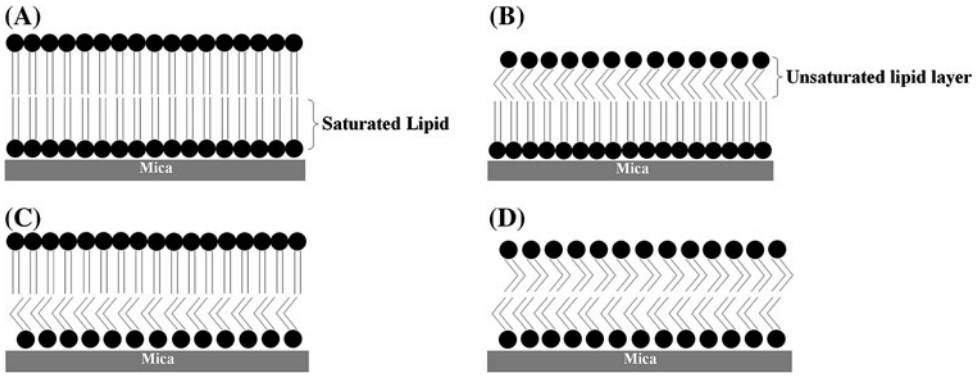

Fig. 2 Schematic drawing of the lipid bilayers composed of individual leaflets that have each phase: **a** solid-like first leaflet and solid-like second leaflet, **b** solid-like first leaflet and liquid-like second leaflet, **c** liquid-like first leaflet and solid-like second leaflet and **d** liquid-like first leaflet and liquid-like second leaflet

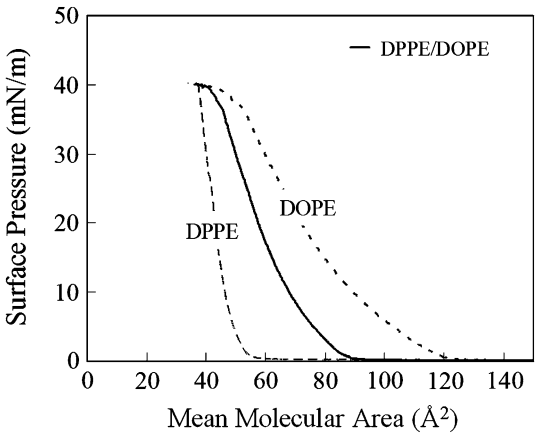

Fig. 3 Surface pressure versus area per molecule isotherms for DPPE, DOPE and mixed (1:1) DPPC/DOPC monolayers at the air–water interface (25°C)

pH 4, after DPPC–DPPG and DOPC–DOPG vesicles were, respectively, fused to form lipid bilayers on each monolayer of DPPE and DOPE above the transition temperature of the lipids. Prior to the measurement, topographic images of the bilayers were acquired. The characteristics of the images were identical. Similar surface forces were expected over the DPPC–DPPG/DOPE and DOPC–DOPG/DPPE bilayers since the layers have identical headgroups and tail lengths. However, the surface force over the DPPC–DPPG/DOPE bilayer was not only different from those over the DPPC–DPPG/DPPE bilayer and DOPC–DOPG/DOPE bilayers but also nonidentical with that over the DOPC–DOPG/DPPE bilayer. First, during the approach the resistance to contact indicative of short-range repulsion was found more for the DPPC–DPPG/DOPE bilayer than for the DOPC–DOPG/DPPE bilayer (Fig. 4a). Second, upon retraction the DOPC–DOPG/DPPE bilayer showed a strong adhesive pull-off force, while there was almost no adhesion on the DPPC–DPPG/DOPE bilayer (Fig. 4b). Surface energy did not appear to account for these features as the second leaflets of both layers had identical headgroups. The features in the force curves indicate that the van der Waals interactions between the DPPC–DPPG/DOPE bilayer and the probe were offset by a strong repulsive force.

Further evidence of a short-range repulsion was observed when the applied load was increased to over 1 nN. While the force curves over the DOPC–DOPG/DPPE bilayer remained unchanged, a completely different force was obtained over the DPPC–DPPG/DOPE bilayer (Fig. 4c). At a surface separation of ~ 1 nm, a steep repulsion could be seen, where the force increases until the probe jumps to contact, indicating a change from a net repulsive to a net attractive force and that the gradient of the force between the probe and the surface had exceeded the spring constant of the cantilever. This repulsion decayed exponentially with distance, with a

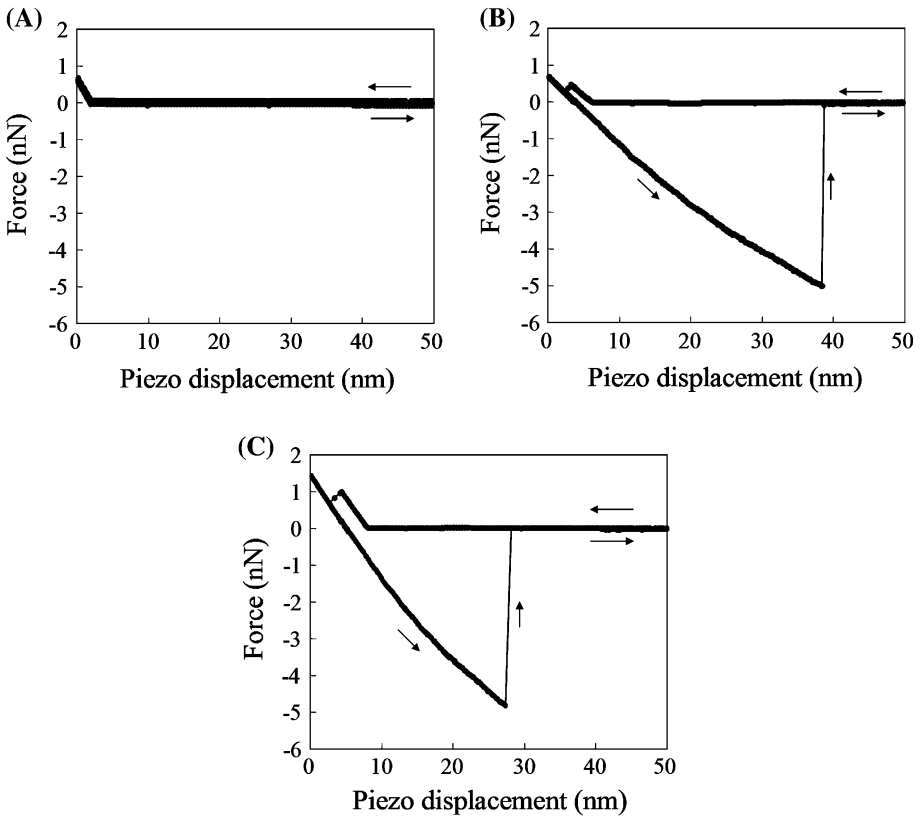

Fig. 4 Force–distance curves recorded over the lipid bilayers at 25°C: **a** DPPC–DPPG/DOPE with 0.7-nN load, **b** DOPC–DOPG/DPPE with 0.7-nN load and **c** DPPC–DPPG/DOPE with 1.5-nN load

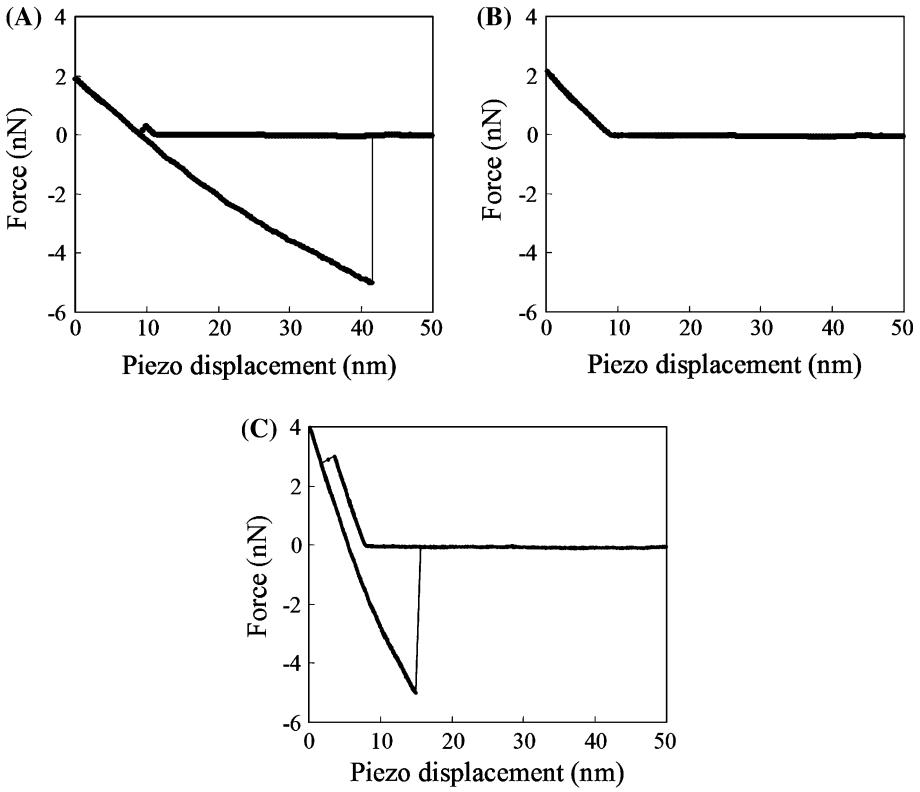

Fig. 5 Force–distance curves recorded over the lipid bilayers at 25°C: **a** DOPC–DOPG/DOPE with 2-nN load, **b** DPPC–DPPG/DPPE with 2-nN load and **c** DPPC–DPPG/DPPE with 4-nN load

decay length of ~0.7 nm, and was indicative of hydration/steric interaction forces, which are consistent with data obtained with the surface forces apparatus on lipid bilayers (Marra and Israelachvili 1985). The snap to contact suggests that the DPPC–DPPG/DOPE headgroups were deformed by ~1-nN loads, resulting in disruption of the structure of the water layer. The results suggest that the lipid layers that had identical tail lengths and headgroups may have different surface forces due to asymmetry of the bilayers. Detailed analysis for this observation is described later.

Several different loads, from 0.5 to 4 nN, were applied to the lipid layers. The force curves over the DPPC–DOPE bilayer remained unchanged at loads over 1 nN, and the force curves over the DOPC–DPPE bilayer remained unchanged at loads over 0.5 nN. The force–distance curves over the DPPC–DPPE and DOPC–DOPE bilayers are shown in Fig. 5. Disruption was found at 3 and 0.3 nN for the DPPC–DPPG/DPPE and DOPC–DOPG/DOPE bilayers, respectively. The loads of the lipid bilayers, which caused the disruption, are summarized in Table 1.

The difference among hydration/steric forces over the bilayers appears to be related to their different mechanical stability under the studied loads. While the saturated lipids (DPPC, DPPG and DPPE) have strong cohesive forces due to strong lateral interactions between the molecules, a lower cohesion/stability is expected for the unsaturated lipids (DOPC, DOPG and DOPE) due to reduced van der Waals interactions between the unsaturated hydrocarbon chains and reduced possibility for hydrogen bonds between the headgroups.

From the results described above, the stability of the second leaflet where the probe was touched had an obvious effect on the surface force. Disruption on the DOPC–DOPG/DPPE bilayer occurred at a lower load than that on

Table 1 Short-range repulsions and adhesions on the lipid bilayers

	DPPC–DPPG leaflet		DOPC–DOPG leaflet	
	First DPPE leaflet	First DOPE leaflet	First DPPE leaflet	First DOPE leaflet
Short-range repulsion	~3 nN	~1 nN	~0.5 nN	~0.3 nN
Adhesion				
Less than 1-nN load	No adhesion	No adhesion	~5 nN	~5 nN
Less than 2-nN load	No adhesion	~5 nN	~5 nN	~5 nN
Less than 4-nN load	~5 nN	~5 nN	~5 nN	~5 nN

the DPPC–DPPG/DPPE bilayer. In addition, it was found that the force curve shape was determined not only by the second-leaflet structure but also by the first-leaflet structure. The resistance to contact for the DPPC–DPPG/DPPE bilayer was much larger than that for the DPPC–DPPG/DOPE bilayer. The disruption load values of the DPPC–DPPG/DPPE, DPPC–DPPG/DOPE and DOPC–DOPG/DOPE bilayers were compared. Since the disruption load of the DOPC–DOPG/DOPE bilayer was $\sim$0.3 nN, the disruption load of the DPPC–DPPG/DOPE bilayer, $\sim$1 nN, appears to be used to deform mainly the DPPC–DPPG leaflet. However, the disruption load of the DPPC–DPPE bilayer was $\sim$3 nN, which was apparently the force to disrupt mainly the DPPC–DPPG leaflet and sequentially the DPPE leaflet. In other words, if a load disrupted the DPPC–DPPG leaflet, the amplitude of the load was also enough to disrupt the DPPE leaflet. The reason is that DPPC–DPPG and DPPE have identical chain lengths of tailgroups and the mechanical stability was known to depend on the tailgroups of the lipid layer, not the headgroups of the layer (Park and Ahn 2008). In other words, it may be claimed that the disruption of the DPPC–DPPG leaflet on the DOPE leaflet was caused with a 1-nN load while the disruption of the DPPC–DPPG leaflet on the DPPE leaflet was with a 3-nN load. This finding means that the first-leaflet structure seemed to affect the second-leaflet structure.

From comparison of the surface forces between the DPPC–DPPG/DOPE and the DOPC–DOPG/DPPE bilayers, the second-leaflet structure where the probe touched appears to be important. Both the DPPC–DPPG/DOPE and the DOPC–DOPG/DPPE bilayers have identical components—carbon numbers and headgroups. However, as described above, disruption of the DPPC–DPPG/DOPE bilayer occurred at a higher load than that of the DOPC–DOPG/DPPE bilayer. This result indicates that the second-leaflet structure where the probe touched at first appears to be crucial for the surface force which shows short-range repulsion. The headgroup structure is also related to the mechanical stability of the second leaflet. Therefore, the DPPC–DPPG leaflet seems to be more stable than the DOPC–DOPG leaflet, even though the DPPC–DPPG leaflet was formed on the DOPE leaflet. The findings described above, that hydration/steric repulsion over lipid bilayers depends on their mechanical stability and asymmetry, are of biological relevance in the control of cell adhesion and membrane fusion processes.

For a more quantitative characterization of the lipid bilayer surface properties, the surface charge density and potential of the 3-μm-diameter silica sphere were found first, with the force measurements between the sphere and the silica surface. Figure 6 shows the approaching surface force measurements as a function of the separation between

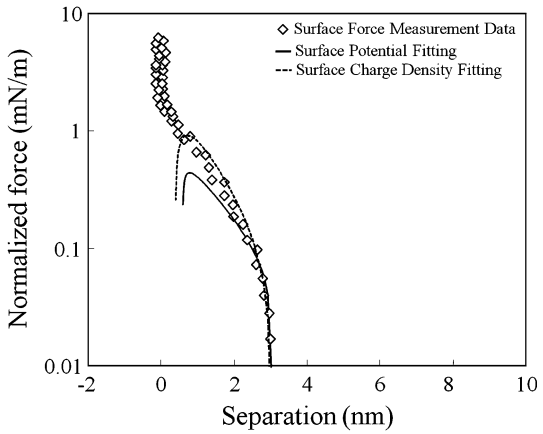

Fig. 6 Approaching force curve as a function of the separation between the silica surfaces in 300 mM sodium chloride at pH 4

the silica sphere and the silica surface in 300 mM sodium chloride at pH 4. The long-range surface forces were purely repulsive. The exponential dependence of the repulsive force on distance was consistent with double-layer forces between surfaces of like charge in aqueous solutions. At separations of less than 2 nm, significant short-range repulsive forces were observed that may be attributed to the steric forces (Horn et al. 1989; Ducker et al. 1991).

The DLVO theory was applied to analyze the long-range surface forces using either constant surface potential or charge density boundary conditions. The surface potential of the silica surface was -14 ± 1 mV, and the surface charge density was $-20 \pm 1 \times 10^{-3}$ C/m^2. Our results appear to be consistent with those of Park and Lee (2006), where AFM was used to characterize the charge state of the silica surface in 1, 10 and 100 mM sodium chloride solutions and the surface potential was found to be in the range of -50 to -20 mV at pH 4. For the purpose of this study, the experimentally measured silica surface potential and

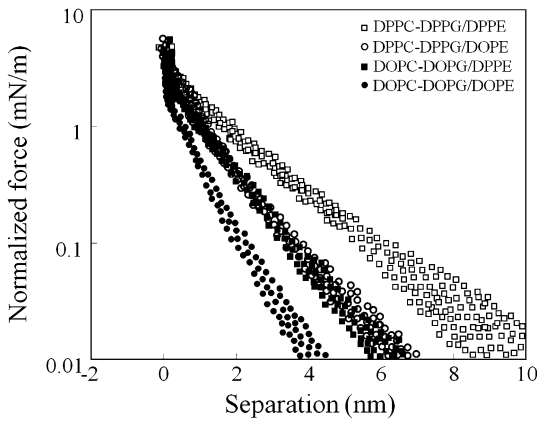

Fig. 7 Approaching force curves as a function of the separation between the silica sphere and the lipid bilayer in 300 mM sodium chloride at pH 4

Table 2 Surface potentials and charge densities measured on the lipid bilayers as a function of the components

	DPPC–DPPG leaflet		DOPC–DOPG leaflet	
	First DPPE leaflet	First DOPE leaflet	First DPPE leaflet	First DOPE leaflet
Surface potential (mV)	-66 ± 5	-35 ± 3	-33 ± 3	-18 ± 2
Surface charge density (10^{-3} C/m^2)	-90 ± 6	-48 ± 4	-45 ± 3	-25 ± 2

charge density were used to characterize the surface properties of the lipid bilayers.

The surface potential and charge density of the lipid bilayers were characterized by making surface force measurements on them with the silica sphere. Figure 7 shows the results of force measurements made on the lipid bilayers in 300 mM sodium chloride at pH 4. The long-range surface forces were purely repulsive and varied with the components of the lipids that were used for the preparation of the vesicles. Quantitative analysis of the surface forces with the DLVO theory was performed using asymmetric boundary conditions. Table 2 summarizes the surface potentials and charge densities measured on the lipid bilayers as a function of the components. It was observed that the surface charge densities and potentials of the lipid bilayer were much larger than those for the silica surfaces, which can be attributed to the ionic lipid component of the lipid bilayer. It was noted that the electrostatic properties of the DPPC–DPPG/DOPE and the DOPC–DOPG/DPPE bilayers were almost identical while the adhesion and the steric/hydration repulsion were different. Also, the surface charge densities and potentials were higher with greater density of the lipid bilayer, which led to a more stable bilayer.

Conclusion

Lipid monolayers exhibiting different phases were used as the first leaflets where the second leaflets were formed. After the formation of the lipid bilayers, the effect of their mechanical stability on the nanometer-scale physical properties was investigated. The unique force to disrupt each bilayer was found, and their characteristic pull-off adhesion forces were measured. Furthermore, the electrostatic properties of the bilayers were evaluated. This study demonstrates the important role that mechanical properties play in the surface behavior of phospholipid bilayers.

Acknowledgments This work was supported by the Basic Science Research Program through the National Research Foundation of Korea (NRF) funded by the Ministry of Education, Science and Technology (2010-0010097). We thank all of the members of the Department of Chemical Engineering, Seoul National University of Technology, for help and valuable discussions. We thank Prof. I. S. Yoo at Kyungwon University and Prof. D. J. Ahn, Dr. G. S. Lee, Mr. H. Choi and Mr. C. S. Choi at Korea University for valuable help.

References

Bagatolli LA, Gratton E (2000) A correlation between lipid domain shape and binary phospholipid mixture composition in free standing bilayers: a two-photon fluorescence microscopy study. Biophys J 79:434–447

Beech B, Smith JR, Steele AA, Penegar I, Campbell SA (2002) The use of atomic force microscopy for studying interactions of bacterial biofilms with surfaces. Colloids Surf B 23:231–247

Biggs S (1995) Steric and bridging forces between surfaces fearing adsorbed polymer—an atomic-force microscopy study. Langmuir 11:156–162

Boon JM, Smith BD (2002a) Synthetic membrane transporters. Curr Opin Chem Biol 6:749–756

Boon JM, Smith BD (2002b) Chemical control of phospholipid distribution across bilayer membranes. Med Res Rev 22:251–281

Boxer SG (2000) Molecular transport and organization in supported lipid membranes. Curr Opin Chem Biol 4:704–709

Brian AA, McConnell HM (1984) Allogeneic stimulation of cytotoxic T-cells by supported planar membranes. Proc Natl Acad Sci USA 81:6159–6163

Brown DA, London E (2000) Structure and function of sphingolipid- and cholesterol-rich membrane rafts. J Biol Chem 275:17221–17224

Butt H-J, Franz V (2002) Rupture of molecular thin films observed in atomic force microscopy. I. Theory. Phys Rev E 66:031601

Cappella B, Dietler G (1999) Force–distance curves by atomic force microscopy. Surf Sci Rep 34:1–104

Chan DYC, Pashley RM, White LR (1980) A simple algorithm for the calculation of the electrostatic repulsion between identical charged surfaces in electrolyte. J Colloid Interface Sci 77:283–285

De Almeida RFM, Loura LMS, Fedorov A, Prieto M (2002) Nonequilibrium phenomena in the phase separation of a two-component lipid bilayer. Biophys J 82:823–834

Derjaguin BV (1934) Analysis of friction and adhesion IV. The theory of the adhesion of small particles. Kolloid Z 69:155–164

Derjaguin BV (1940) On the repulsive forces between charged colloid particles and on the theory of slow coagulation and stability of lyophobe sols. Trans Faraday Soc 36:203–211

Devaux PF, Morris R (2004) Transmembrane asymmetry and lateral domains in biological membranes. Traffic 5:241–246

Dimitriadis EK, Horkay F, Maresca J, Kachar B, Chadwick RS (2002) Determination of elastic moduli of thin layers of soft material using the atomic force microscope. Biophys J 82:2798–2810

Ducker WA, Senden TJ, Pashley RM (1991) Direct measurement of colloidal forces using an atomic force microscope. Nature 353:239–241

Ducker WA, Senden TJ, Pashley RM (1992) Measurement of forces in liquids using a force microscope. Langmuir 8:1831–1836

Engler AJ, Richert L, Wong JY, Picart C, Discher DE (2004) Surface probe measurements of the elasticity of sectioned tissue, thin gels and polyelectrolyte multilayer films: correlations between substrate stiffness and cell adhesion. Surf Sci 570:142–154

Fang HH, Chan PK-Y, Xu L-C (2000) Quantification of bacterial adhesion forces using atomic force microscopy (AFM). J Microbiol Methods 40:89–97

Franz V, Loi S, Muller H, Bamberg E, Butt H-J (2002) Tip penetration through lipid bilayers in atomic force microscopy. Colloids Surf B 23:191–200

Garcia-Manyes S, Oncins G, Sanz F (2005) Effect of ion-binding and chemical phospholipid structure on the nanomechanics of lipid bilayers studied by force spectroscopy. Biophys J 89:1812–1826

Giesen PL, Willems GM, Hemker HC, Hermens WT (1991) Membrane-mediated assembly of the prothrombinase complex. J Biol Chem 266:18720–18725

Hartmann U (1991) Van der Waals interactions between sharp probes and flat sample surfaces. Phys Rev B 43:2404–2407

Hogg R, Healy TW, Fuersten DW (1966) Mutual coagulation of colloidal dispersions. Trans Faraday Soc 62:1638–1651

Horn RG, Smith DT, Haller W (1989) Surface forces and viscosity of water measured between silica sheets. Chem Phys Lett 162: 404–408

Hunter RJ (1987) Foundations of colloid science. Oxford University Press, Oxford

Israelachvili JN (1991) Intermolecular and surface forces. Academic Press, New York

Israelachvili JN, Adams GE (1978) Measurement of forces between 2 mica surfaces in aqueous-electrolyte solutions in range 0–100 nm. J Chem Soc Faraday Trans 74:975–1001

Loi S, Sun G, Franz V, Butt H-J (2002) Rupture of molecular thin films observed in atomic force microscopy. II. Experiment. Phys Rev E 66:031602

Marra J, Israelachvili JN (1985) Direct measurements of forces between phosphatidylcholine and phosphatidylethanolamine bilayers in aqueous-electrolyte solutions. Biochemistry 24:4608–4618

McConnell HM, Watts TH, Weis RM, Brian AA (1986) Supported planar membranes in studies of cell–cell recognition in the immune system. Biochim Biophys Acta 864:95–106

Miszta A, Machan R, Benda A, Ouellette AJ, Hermens WT, Hof M (2008) Combination of ellipsometry, laser scanning microscopy and Z-scan fluorescence correlation spectroscopy elucidating interaction of cryptdin-4 with supported phospholipid bilayers. J Pept Sci 14:503–509

Mou JX, Yang J, Huang C, Shao Z (1994) Alcohol induces interdigitated domains in unilamellar phosphatidylcholine bilayers. Biochemistry 33:9981–9985

O'Shea SJ, Welland ME, Pethica JB (1994) Atomic-force microscopy of local compliance at solid–liquid interfaces. Chem Phys Lett 223:336–340

Park J-W (2007) Nanoliter reactor arrays for antibiotic study. Bull Korean Chem Soc 28:1709–1714

Park J-W, Ahn DJ (2008) Temperature effect on nanometer-scale physical properties of mixed phospholipid monolayers. Colloids Surf B 62:157–161

Park J-W, Lee GU (2006) Properties of mixed lipid monolayers assembled on hydrophobic surfaces through vesicle adsorption. Langmuir 22:5057–5063

Parker JL (1994) Surface force measurements in surfactant systems. Prog Surf Sci 3:205–271

Parker JL, Christenson HK (1988) Measurements of the forces between a metal-surface and mica across liquids. J Chem Phys 88:8013–8014

Rinia HA, Snel MME, van dern Eerden JPJM, de Kruijff B (2001) Visualizing detergent resistant domains in model membranes with atomic force microscopy. FEBS Lett 501:92–96

Sackmann E (1996) Supported membranes: scientific and practical applications. Science 271:43–48

Senden TJ, Drummond CJ, Kékicheff P (1994) Atomic-force microscopy—imaging with electrical double-layer interactions. Langmuir 10:358–362

Shuin V, Kekicheff P (1993) Electrical double-layer structure revisited via a surface force apparatus—mica interfaces in lithium-nitrate solutions. J Colloid Interface Sci 155:108–123

Tokumasu F, Jin AJ, Feigenson GW, Dvorak JA (2003) Characterization of micro-domain structure in ROS disk model membranes using differential scanning calorimetry and atomic force microscopy. Biophys J 84:2609–2618

Van der Vegte EW, Hadziioannou G (1997) Scanning force microscopy with chemical specificity: an extensive study of chemically specific tip–surface interactions and the chemical imaging of surface functional groups. Langmuir 13:4357–4368

Verwey EJW, Overbeek JTG (1948) Theory of the stability of lyophobic colloids. Elsevier, New York